ORIGINAL ARTICLE

Bridging the structure gap between pellets in artificial dissolution media and in gastro-intestinal tract in rats

Hongyu Sun[a,b,†], Siyu He[b,c,†], Li Wu[b], Zeying Cao[b,c], Xian Sun[b,c,h], Mingwei Xu[g], Shan Lu[b,d], Mingdi Xu[f], Baoming Ning[f], Huimin Sun[e,f], Tiqiao Xiao[g], Peter York[b], Xu Xu[a,*], Xianzhen Yin[b,h,*], Jiwen Zhang[a,b,e,*]

[a]School of Chemical and Environmental Engineering, Shanghai Institute of Technology, Shanghai 201418, China
[b]Center for Drug Delivery System, Shanghai Institute of Materia Medica, Chinese Academy of Sciences, Shanghai 201210, China
[c]University of Chinese Academy of Sciences, Beijing 100049, China
[d]School of Materials Science and Engineering, Center for Supramolecular Chemistry and Catalysis, Department of Chemistry, Shanghai University, Shanghai 200444, China
[e]NMPA Key Laboratory for Quality Research and Evaluation of Pharmaceutical Excipients, National Institutes for Food and Drug Control, Beijing 100050, China
[f]National Institutes for Food and Drug Control, Beijing 100050, China
[g]Shanghai Synchrotron Radiation Facility/Zhangjiang Lab, Shanghai Advanced Research Institute, Chinese Academy of Sciences, Shanghai 201204, China
[h]Center for MOST and Image Fusion Analysis, Shanghai Institute of Materia Medica, Chinese Academy of Sciences, Shanghai 201210, China

Abstract   Changes in structure of oral solid dosage forms (OSDF) elementally determine the drug release and its therapeutic effects. In this research, synchrotron radiation X-ray micro-computed tomography was utilized to visualize the 3D structure of enteric coated pellets recovered from the gastrointestinal tract of rats. The structures of pellets in solid state and *in vitro* compendium media were measured.

---

*Corresponding authors. Tel./fax: +86 21 50805901 (Jiwen Zhang); +86 21 50805622 (Xianzhen Yin); +86 21 60873372 (Xu Xu).
    E-mail addresses: xuxu3426@sina.com (Xu Xu), xzyin@mail.shcnc.ac.cn (Xianzhen Yin), jwzhanggroup@163.com, jwzhang@simm.ac.cn (Jiwen Zhang).
    †These authors made equal contributions to this work.

Pellets *in vivo* underwent morphological and structural changes which differed significantly from those *in vitro* compendium media. Thus, optimizations of the dissolution media were performed to mimic the appropriate *in vivo* conditions by introducing pepsin and glass microspheres in media. The sphericity, pellet volume, pore volume and porosity of the *in vivo* esomeprazole magnesium pellets in stomach for 2 h were recorded 0.47, 1.55×10^8 μm^3, 0.44×10^8 μm^3 and 27.6%, respectively. After adding pepsin and glass microspheres, the above parameters *in vitro* reached to 0.44, 1.64×10^8 μm^3, 0.38×10^8 μm^3 and 23.0%, respectively. Omeprazole magnesium pellets behaved similarly. The structural features of pellets between *in vitro* media and *in vivo* condition were bridged successfully in terms of 3D structures to ensure better design, characterization and quality control of advanced OSDF.

1. Introduction

The structural fates of oral solid dosage forms (OSDF) during drug dissolution/release either *in vitro* or *in vivo* are largely uncovered in most cases. Once the OSDF are administered, structural dynamics decides their release profiles and hence, their therapeutic effects. Therefore, tracking the *in vivo* structural changes could be of great importance. Previously, few *in vivo* structural studies on OSDF lead to the question of whether the widely used *in vitro* drug dissolution/release test aids the design of OSDF without any linkage to *in vivo* structural changes. Linking *in vivo* structural changes of OSDF to *in vitro* measurements could be very helpful in quality control and the design and development of advanced OSDF[1]. Imaging is a crucial and direct technique to observe the structure of OSDF. There are a number of methods to evaluate three-dimensional (3D) structural performance of OSDF, including nuclear magnetic resonance imaging[2,3], confocal laser scanning microscopy[4], Terahertz imaging[5], 3D Scanning electron microscope[6] and stimulated Raman scattering microscopy[7]. However, most of them are unable to effectively characterize the internal microstructure due to weak penetration of dosage forms and low resolution of the imaging apparatus. Most of the reported studies on OSDF structural changes have been focused on simple *in vitro* observations which are not indicative of *in vivo* structural profiles. X-ray imaging and optical coherence tomography can provide the details of internal fine structures[8,9] and has the potential to resolve internal structures of OSDF and other medicinal preparations.

Synchrotron radiation X-ray micro computed tomography (SR-μCT) has shown promising results in resolving the internal structures and material distribution in wide range of structures. Although medical X-ray CT has long been used to study the internal structures, the X-ray produced by the Synchrotron light source is benefitted from highly collimated and monochromatic light. SR-μCT is a powerful tool in the quantitative structure research of dosage forms as well as particles of pharmaceutical excipients[10−12]. The 3D morphology of a number of preparations, microspheres[13], tablets[14,15], crystals and granules[16] have been successfully evaluated non-invasively, using SR-μCT. In addition, the dynamic structure of OSDF has also been studied using SR-μCT[17]. For example, the drug release kinetics and quantification of swelling and erosion in the controlled release tablets were investigated. The mechanism of controlled drug release and pellet structure variation were correlated *via* a single pellet observation strategy[18]. An SR-μCT microstructural characterization combined with chemical determination approach for formulation development of material distribution in multiple-unit pellet system tablet was developed[19]. Furthermore, the relationship between the structure of sustained-release pellets in metoprolol succinate sustained-release tablets and drug release was also established[20]. However, all these researches focused only on *in vitro* structural changes of OSDF and their *in vivo* fate remained undiscovered. Therefore, studies of the real-time structural architectures of OSDF *in vivo* are a critically important domain for research. It is of great significance to explore the structure performance of OSDF *in vivo*.

The pellets are suitable for the measurements using SR-μCT because of their appropriate particle size. Tablets compressed of enteric coated pellets provide a multiple unit pellet system with special preparation processes[21] and unique release characteristics[22−26]. Coating provides safe passage through highly acidic environment in stomach and help them release at higher pH in gastrointestinal tract[27]. The enteric coated pellets compressed into tablets are the primary units to determine whether a favorable therapeutic effect can be achieved. In this study, esomeprazole magnesium (ESO) enteric coated pellets and omeprazole magnesium (OME) enteric coated pellets were selected as model formulations. *In-situ* nondestructive method, SR-μCT, was employed to investigate the structural variations in pellets isolated from the gastro-intestinal tract of rats. The structures of the same pellets from *in vitro* compendium media adopted by Chinese Pharmacopoeia were measured and assessed as well. It is interesting to note that the structure of ESO and OME pellets underwent different changes, which were not consistent between *in vitro* compendium media and *in vivo* conditions. When the structural integrity of the pellets was destroyed or altered, the dissolution behavior of the pellets will certainly change. Therefore, the dissolution behavior of *in vivo* pellets is different from that of *in vitro* pellets due to their different structure fates. The discordance of *in vivo* and *in vitro* dissolution behaviors of pellets can be evaluated from the structure because there was no way to directly measure it *in vivo*. Thus, the structural consistency was the bridge linking the dissolution behavior of the pellets *in vitro* and *in vivo*. Herein, to simulate more realistic *in vivo* physiological conditions, optimization of the dissolution conditions *in vitro* was carried out by adding enzymes and introducing mechanical forces to the surface of the pellets directly. As a result, the structure of pellets *in vivo* and *in vitro* can be better correlated by adjusting the dissolution conditions. Through reconstruction and quantification to the images, the structural differences of enteric pellets in the drug dissolution/release phases *in vivo* and *in vitro* were identified. This research provides a new idea for the reverse engineering and

development of the formulation process by analyzing the structure of pellets both *in vivo* and *in vitro*. Meanwhile, by optimizing the dissolution medium of enteric-coated pellets *in vitro*, the quality control of enteric-coated pellets can be effectively guided.

2. Materials and methods

2.1. Materials

Esomeprazole magnesium enteric coated tablets (Nexium®) were purchased from AstraZeneca AB (Wuxi, China, batch number: 2006122). Omeprazole magnesium enteric coated tablets (Losec® multiple unit pellet system) were purchased from AstraZeneca AB (SE-151 85, Södertälje Swedish, batch number: 1912139). Pepsin was purchased from Sinopharm Chemical Reagent Co., Ltd. (Shanghai, China). Glass microspheres (GM, 30 mesh, with a diameter of 600 μm) were obtained from Ningbo Xinou Sand-blasting Machinery Co., Ltd. (Ningbo, China). Precise pH test paper was obtained from Shanghai Macklin Biotechnology Co., Ltd. (Shanghai, China). Sprague−Dawley rats (180−220 g, IACUC Application No. 2018-05-ZJW-18) were supplied from Shanghai Laboratory Animal Center, Chinese Academy of Sciences (Shanghai, China). Hydrochloric acid, sodium dihydrogen phosphate, sodium hydrogen phosphate, sodium hydroxide, ethanol, methanol and acetonitrile of analytical grade were obtained from Sinopharm Chemical Reagent Co., Ltd. (China). Water was purified by a reverse osmosis using Milli-Qs system (Millipore, Bedford, MA, USA).

2.2. Preparation of samples for in vitro and in vivo tests

In vitro compendium media release tests were carried by placing an esomeprazole magnesium enteric coated tablet in 300 mL HCl (pH = 1) at 37 °C with a stirring at 100 rpm ($n = 3$), followed by sampling pellets at 0.5, 1, 1.5 and 2 h, respectively. For the evaluation of pellets architectures and *in vivo* retention, tablets were placed in the 300 mL HCl (pH = 1) and disintegrated individual pellets were harvested. Afterwards, 50 pellets were quickly collected and withdrawn into the stomach infusion needle and administered soon after to the rats *via* gavage. Then rats were sacrificed by dislocation of the vertebral crest after anesthesia and dissected at 0.5, 1, 1.5 and 2 h, respectively. The pellets in stomach were carefully counted and collected. Meanwhile, the pH in rat stomach was recorded with a precise pH test paper. All experimental procedures were executed according to the protocols approved by Chinese Academy of Sciences Animal Care and Use Committee.

The residual liquid of collected samples was gently wiped by a piece of dry filter paper and dried to a constant weight at room temperature in dark. Then, twenty pellets were fixed on pipette tips by a double-sided adhesive tape for SR-μCT analysis. The preparation method of OME pellets was the same as that of ESO pellets.

2.3. Acquisition of 2D internal morphology of pellets

Scanning electron microscopy (SEM, FlexSEM1000) was employed to characterize the morphological changes of the pellets. Before the determination, the pellets were frozen in liquid nitrogen, and then cut in the middle, quickly by a surgical knife to get a smooth cross-section. Afterwards, samples were fixed on the platform with conductive glue by facing the cross-sections upward. The SEM images were collected with the accelerating voltage of 10.0 kV.

2.4. SR-μCT image acquisition of pellets

SR-μCT images were obtained in the beam line BL13W1 at Shanghai Synchrotron Radiation Facility (SSRF), the composition of SR-μCT beam line was shown in Fig. 1. For ESO and OME pellets imaging, samples were fixed on the stage. For every 0.125° rotation of the stage, a projection of the pellets from a charge-coupled device was collected. The obtained projections were magnified by diffraction-limited microscope optics using 4 × magnifications and the raw data were digitalized to an effective pixel size of 1.625 μm (physical pixel size about 6.5 μm). As for the imaging parameters, 18 Kev X-ray energy was used, the exposure time was maintained for 0.5 s and the distance between sample and detector (DSD) was adjusted to 20 cm. For each determination, 1440 projections over a rotation angle of 180° were collected. Furthermore, two blank field images (X-rays pass through the optical path without any sample in position) were collected following each 180-projection collection, and five dark field images were acquired for the correction of electronic noise and background after turning off the X-ray beam.

2.5. 3D structure reconstruction and quantitative analysis

Information about the internal structures of samples using 2D projection image acquired by CT scan was obtained after optimization, denoising, coloring and segmentation, respectively. Based on a series of 2D projection images from different angles, a fast convolution back-projection algorithm was utilized to reconstruct 32-bit slice images. PITRE (phase-sensitive X-ray image processing and tomography reconstruction) was used to reduce the noise and optimize the 32-bit slice image into 8 bit with improved distinction of different material and density regions. During this process, the line profile showed the difference in X-ray absorption of the pellet compositions. Amira software (version 6.01, FEI, USA) was then applied to reconstruct the 3D structure and the cross section of pellets by importing the slice images. Finally, the 3D-Tiff files generated by Amria software were imported into Image Pro Premier software (version 7.0, Media Cybernetics, Inc., USA), and the objects on the complex images were automatically detected by the intelligent segmentation or threshold setting function. Afterwards, the 3D structural parameters of the pellets—sphericity (sphericity of object, calculated as 6 volumes of object divided by equivalent diameter and surface area of object), volume (volume of object in calibrated units) and porosity [following in Eq. (1)] were calculated automatically by Image Pro Premier software.
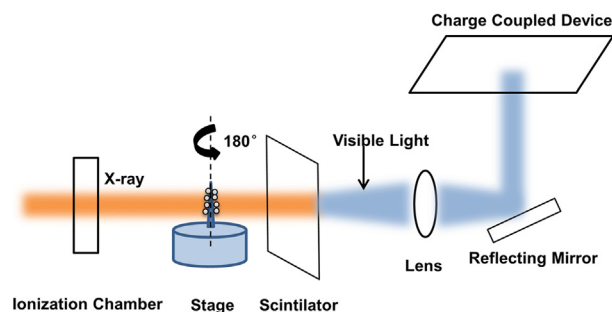

Figure 1   Schematic showing SR-μCT beam line composition.

$$Porosity\ (\%) = \frac{Pore\ volume}{Pellet\ volume} \times 100 \qquad (1)$$

2.6. Alignment of the pellet structures in vivo and in vitro in compendium media

Because of the peristalsis effects and the function of enzymes *in vivo*, the structure changes of pellets presented a marked difference between *in vivo* and *in vitro* compendium media samples. In order to identify the factors on structural variation of pellets in the compendium media and in the actual physiological condition, alternative dissolution parameters such as pepsin or GM were considered. Here, pepsin addition to simulate the gastric environment, GM to imitate stomach motility or adding pepsin mixed GM were evaluated to identify the factors responsible for difference in structural variations between *in vivo* and *in vitro*. The pepsin medium was prepared as follows: 10 g pepsin and 2 g of NaCl were dissolved in 5 mL of HCl (37%, *w/w*) and 995 mL of pure water. Additional 1 mol/L HCl was used to adjust the medium to pH = 1 wherever required. For imitation of peristalsis and friction in the gastrointestinal tract, different amounts of GM were added to the HCl medium (pH = 1) until the GM (c = 50 g/L) was tapered at the bottom of the dissolution vessels and the pellets moved along the top layer of the GM stack after the stirring paddle was turned on. Herein, 15 g of GM were suspended in 300 mL of HCl (pH = 1) as the second modified dissolution media. In addition, a mixture of pepsin and GM as the third modified media was prepared by adding 15 g of GM to the first modified media of 300 mL. The other operations were the same as Section 2.2. Finally, pellets were collected at 0.5, 1, 1.5 and 2 h, respectively. The collected pellets were dried similarly as that of *in vitro* compendium media samples.

2.7. Statistics

Student's *t*-test was performed for comparison of structural parameters between groups. The confidence level was set as significant when $^{*}P < 0.05$ and highly significant when $^{*}P < 0.01$ and $^{*}P < 0.001$. Meanwhile, ns represents no significant difference between two groups. All results were presented as the mean $\pm$ SD.

3. Results and discussion

3.1. Analysis of manufacturing technology for enteric coated pellets

For esomeprazole magnesium and omeprazole magnesium multiple unit pellet systems, the tablets are composed of the active pharmaceutical ingredient (API) and following excipients: glyceryl monostearate, hydroxypropyl methylcellulose, hydroxypropyl cellulose, iron oxide, magnesium stearate, methacrylic acid-ethyl acrylate co-polymer, microcrystalline cellulose, synthetic paraffin, polyethylene glycol, polysorbate 80, polyvinylpyrrolidone, sodium stearyl fumarate, sugar spheres, talc, titanium dioxide, and triethyl citrate[28–30]. The preparation technology for the enteric coated pellets within compressed tablets is complex. The products are designed to ensure that the enteric coated pellets maintain the integrity in the stomach and release the drug in intestine. Firstly, the core materials are prepared using a spray drying or spray congealing technique. The API is then mixed with the binder and

other components (such as surfactant, fillers, disintegrators, alkaline additives or other pharmaceutically acceptable ingredients) and coated on the surface of the cores to form a drug layer. It should be noted that before enteric coating, the core pellets are pre-coated with separation layer to avoid direct contact between the enteric coating and acid-sensitive drugs, avoiding any potential drug degradation. Finally, one or more enteric coating layers are applied onto the core materials covered with drug layers and separating layers. These enteric coated pellets are prepared into tablets which are designed to disintegrate into stomach and pellets release. There were different layers in the preparation process of enteric coated pellets and each layer contained different substances. Therefore, each layer has a different absorption of X-rays which helped in clear visualization by SR-μCT.

3.2. Retention and distribution of pellets in the gastrointestinal tract of rats

It was observed that the enteric coated pellets were only found intact in stomachs as they dissolved when reach intestines in rats. Therefore, the structure measurements were done on the pellets taken from the stomach. The retention of ESO and OME pellets in stomachs are shown in Tables 1 and 2, respectively. Results demonstrated that the retention rate (%) of ESO pellets (the number of pellets in stomach/pellets within intra-gastric administration × 100) was 38.97 $\pm$ 9.60% and most of the pellets had passed into the intestines 2 h after administration. The retention and distribution of OME pellets in the stomach were found to be in close agreement with those for ESO pellets. The retention of OME pellets in stomach accounted for 40.36 $\pm$ 7.09% after 2 h of administration. Furthermore, a significant change in color for both types of pellets was noticed. The observed dark color of the pellets could be attributed to chemical degradation of the respective drug substances. The pH of the fluid in rat stomachs were measured to be in the range of 1−2 which was comparable to the one used for *in vitro* (pH = 1) measurements. Overall, the obtained values suggested the fair comparison between the samples treated *in vivo* and *in vitro*.

3.3. In vitro structure of pellets in compendium media by 2D imaging

To explore the structural transformation of enteric coated pellets during the *in vitro* dissolution process, pellets from acidic media (pH = 1) were harvested and imaged at different time intervals. As an initial rapid imaging, SEM was used to track the apparent morphological changes. As shown in Fig. 2A, large holes appeared at the central area after 0.5 h followed by the formation of more cavities at 1 h. The increased gaps/holes with time lead to structural collapse at final stage after 2 h. The similar trend of

Table 1 The gastric retention ESO pellets (%) after oral administration of enteric coated pellets in rats.

T (h)	Pellet recovered in stomach (%)	Surface color of pellets
0.5	94.64 $\pm$ 1.40	White
1.0	77.20 $\pm$ 4.88	Pink
1.5	57.67 $\pm$ 1.70	Lilac
2.0	38.97 $\pm$ 9.60	Purple

Data were presented as means $\pm$ SD, n = 3.

Table 2   The gastric retention of OME pellets (%) after oral administration of enteric coated pellets in rats ($n = 3$).

T (h)	Pellet recovered in stomach (%)	Surface color of pellets
0.5	96.37 ± 0.92	White
1.0	80.03 ± 3.69	Pink
1.5	64.72 ± 1.90	Lilac
2.0	40.36 ± 7.09	Purple

Data were presented as means ± SD, $n = 3$.

structural changes was observed for OME tablets (Fig. 2C). With increased dissolution time, the voids and holes inside the pellets became larger and small cavities emerged, leading to the loose structure.

3.4.   In vivo structure of pellets in SD rat stomachs by 2D imaging

Samples collected from *in vivo* were also imaged using SEM. Interestingly, pellets recovered from rat stomachs displayed diverse structural characteristics, different from the samples treated in compendium media. For ESO pellets (Fig. 2B), large holes emerged at the center of the pellets at 0.5 h, an observation similar to the 1 h *in vitro* samples. At 1 h, the structure started to collapse, resulting in loss of pellet sphericity. For the samples collected after 2 h, the intact pellet structure disappeared and approximately half of the original volume remained. The differences between the *in vivo* and *in vitro* compendium media samples were also observed for OME pellets (Fig. 2D). At 0.5 h, significantly large holes appeared at the edge in addition to the central holes. The structure collapsed at 1.5 h resulting in total loss of sphericity, 30 min faster when compared to *in vitro* measurements.

3.5.   SR-µCT reconstructed 3D structure of ESO pellets in vitro and in vivo

SR-µCT was applied to visualize the *in situ* 3D structure of the ESO pellets non-invasively (Fig. 3). Twenty pellets were examined for all samples obtained at each time point, and 4 pellets were

randomly selected from the presentation after 3D reconstruction. In SR-µCT imaging, all the typical layers in the pellets were clearly identified. The results of *in vitro* dissolution revealed that cavities formed between the enteric coating layer and the separation layer, and the pellet core was partially dissolved within 0.5 h (Fig. 3A). With further dissolution of the sucrose cores, the size of voids and cavities increased with time. Most importantly, reduced thickness of separation layer *in vitro* compendium medium leads to clear gap between drug and separation layer. After 2 h, the separation layer and sucrose core were eroded and the drug layer deformed, indicating the partial penetration of compendium medium through enteric coating to the center of pellets. The double protection of the enteric coating layer and the separation layer for the drug layer were observed.

Interestingly, pellets showed diverse structure performance in the gastrointestinal tract of rats compared with those from compendium media. The 3D reconstructions (Fig. 3B) demonstrate the details of the structural changes. The effect of stomach fluid penetrated the pellets could be clearly estimated from the size and distribution of pores formed. The disintegration of enteric coating layer after 2 h could be attributed to the gastric acid through the pores in the coating film.

Cavities were formed between the enteric and separating layers at 0.5 h which allowed the gastric acid to pass through and reach the cores to cause erosion. Swelling of the enteric coating layer was more than that of the separating coating layer observed from the reconstructed structures. With additional gastric acid diffusing into the pellets, the pore volume continued to increase at 1 h. Pellets appeared to be squeezed by stomach up to 1.5 h, and the enteric coating layer remained intact. However, unlike *in vitro* samples, the enteric coating layer disintegrated at 2 h and hence lost their sphericity.

3.6.   SR-µCT reconstructed 3D structure of OME pellets in vitro and in vivo

Structural differences could be clearly observed from obtained *in vitro* and *in vivo* data for OME pellets presented in Fig. 4. The sphericity of OME pellets deteriorated much faster *in vivo* when
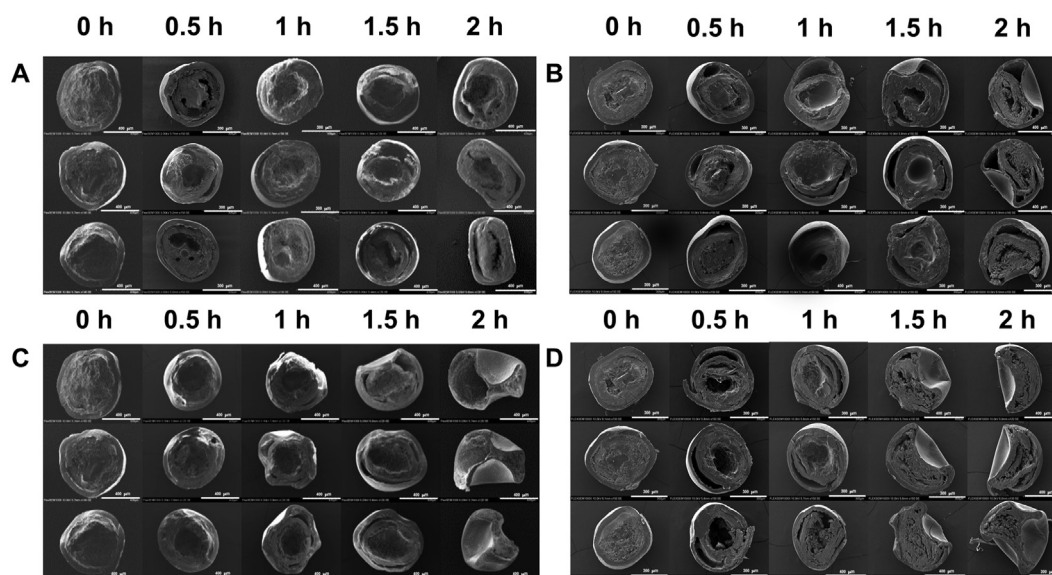

Figure 2   The 2D structure of ESO and OME pellets at different dissolution time *in vitro* and *in vivo* via SEM. (A) ESO pellets *in vitro* compendium media. (B) OME pellets *in vitro* compendium media. (C) ESO pellets *in vivo*. (D) OME pellets *in vivo*.

compared with the samples from *in vitro*. However, unlike ESO pellets, the enteric coating layer remained intact.

It could be clearly observed that when the pellets were exposed to hydrochloric acid for 0.5 h *in vitro* or *in vivo*, the pellets core was partially dissolved, and the pores appeared between the enteric coating layer and the separation layer. The acidic medium could enter the pellets, indicating that the acid sensitive drug omeprazole magnesium had been in contact with hydrochloric acid. The pellets cores dissolved with time and the gaps between coating layers increased initially and then decreased indicated the loss of functionality of enteric coatings. It is concluded that the structure of OME pellets *in vivo* was squeezed more visibly than *in vitro* samples.

3.7. Bridging the structures of pellets in vitro and in vivo

As shown and explained in above sections, there are clear differences between the samples collected from *in vitro* compendium media and *in vivo*. It could be stated that a better *in vitro* dissolution method is needed to accurately simulate the *in vivo* conditions. The structures of pellets undergo through series of structural variations which can significantly influence the drug release and hence the efficacy of the OSDF. Thus, the structural consistency was used as a criterion to evaluate the optimized *in vitro* dissolution method. The physiological environment *in vivo* is much more complex than that of *in vitro* dissolution. However, in the conventional *in vitro* dissolution tests, only pH adjustment is being used to imitate the stomach/intestine environments and the presence of proteases and mechanical peristalsis ignored. Thus, pepsin and GM were introduced to the dissolution medium for bridging the structure variation of pellets *in vitro* and *in vivo*. Surprisingly, as indicated by SEM (Fig. 5) and reconstruction results of ESO (Fig. 6) and OME (Fig. 7) pellets, the structural performance of the pellets was approximately the same as that of the pellets *in vivo* after introducing pepsin to the compendium dissolution media. Possibly, pepsin could be able to break down the proteins in shellac and gelatin in the enteric coating and therefore, allowed more medium to reach pellets cores. Finally, the enteric coating layer was corroded and deformed, which resulted the accelerated structural variation as observed *in vivo*. The addition of GM further reduced the structural differences between *in vitro* and *in vivo*, illustrating the importance of
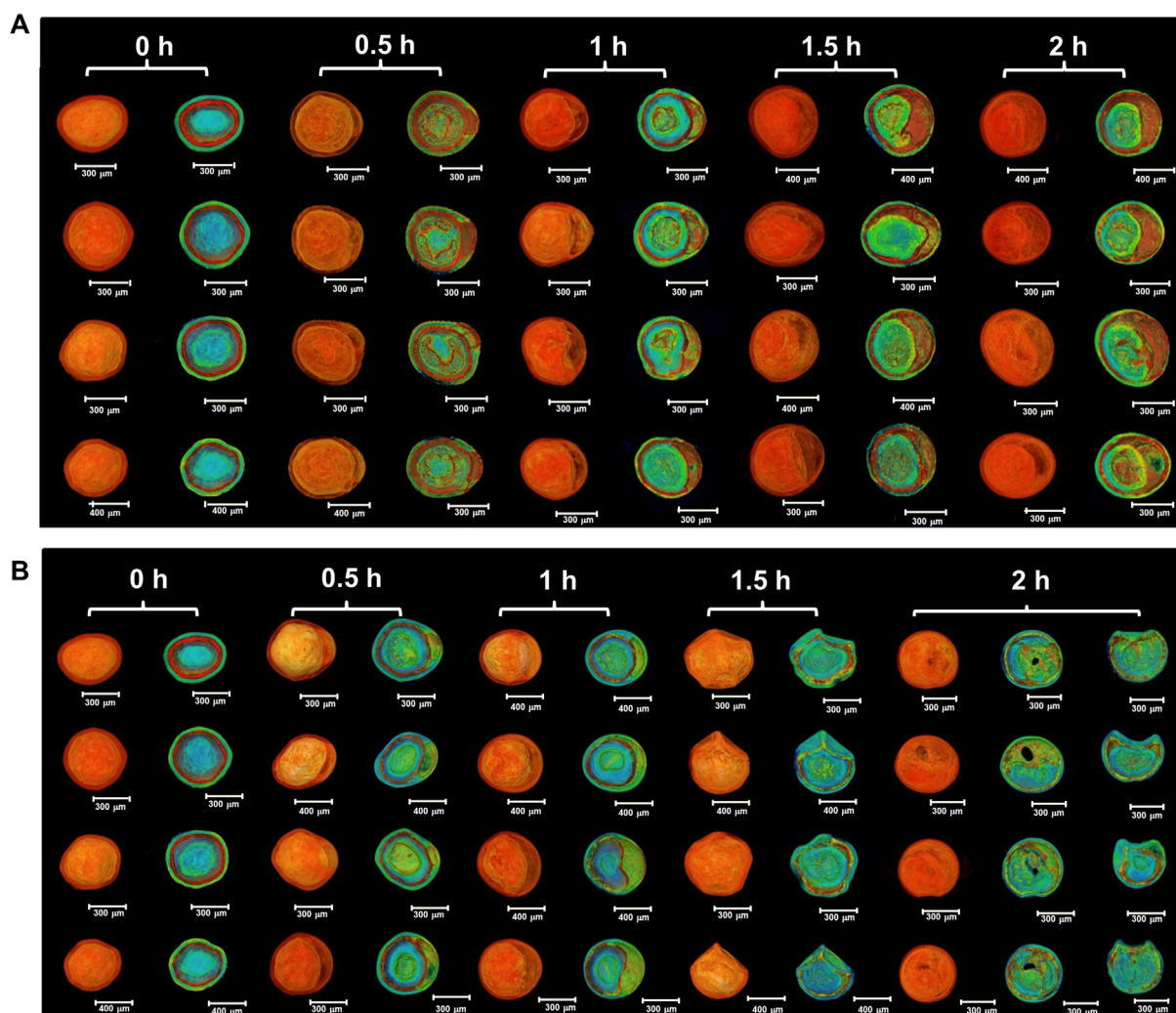

Figure 3　SR-μCT reconstructed 3D structure of ESO pellets with different dissolution times. (A) Structure of ESO pellets at different time points under dissolution condition *in vitro*. Each time point contains two types of images: the transparent outer surface of the pellets (orange color) and the internal cross section of the pellets (multiple colors). (B) Structure of ESO pellets at different time points under dissolution condition *in vivo*. Each time point contains two types of images: the transparent outer surface of the pellets and the internal cross section of the pellets.
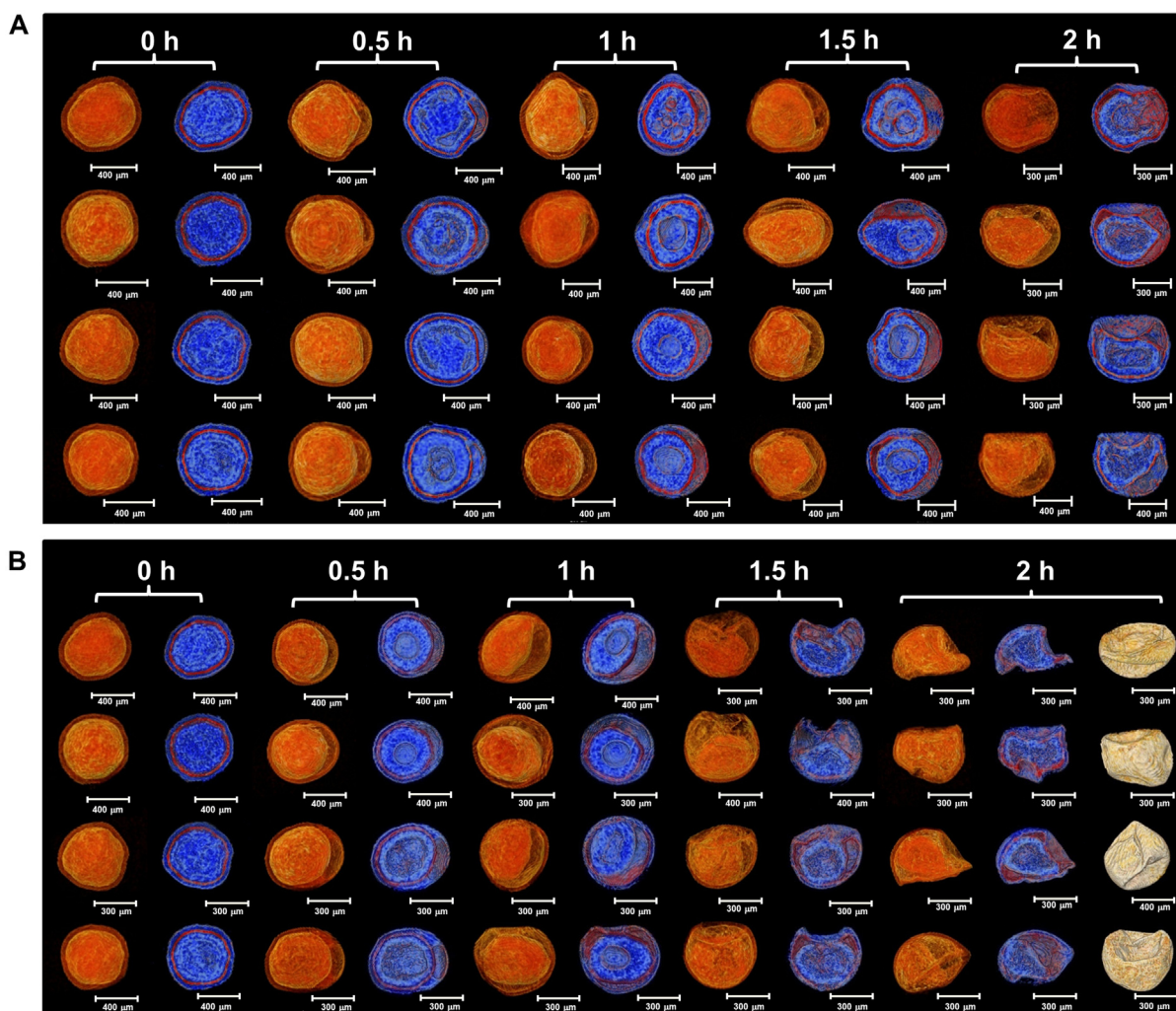
Figure 4   SR-μCT reconstructed 3D structure of OME pellets with different dissolution times. (A) Structure of OME pellets at different time points under dissolution condition *in vitro*. Each time point has two types of images: the transparent outer surface of the pellets (orange color) and the internal cross section of the pellets (multiple colors). (B) Structure of OME pellets at different time points under dissolution condition *in vivo*. Each time point has two types of images: the transparent outer surface of the pellets and the internal cross section of the pellets.

mechanical forces. More importantly, the mixture of pepsin and GM group acted synergistically and structure of pellets altered to same level to that of pellets treated *in vivo*. Therefore, not only the effect of gastrointestinal pH, but also the biological enzymes and mechanical peristalsis should be considered for the *in vitro* dissolution tests. It could be concluded that the pellets structure of ESO tablets and OME tablets *in vitro* were bridged to that of *in vivo* pellets when pepsin and GM were added to the *in vitro* compendium media. And the optimized dissolution method can better simulate the *in vivo* release of the enteric preparation for the OSDF quality control (the structures of the pellets at 2 h were shown more visually in Supporting Information Figs. S1 and S2).

3.8.   Quantitative analysis of structural parameters

Although imaging is a direct method to track the changes in pellets structure, quantitative analysis is very important for better conclusion. Quantitative parameters of 3D structure are very crucial for pellet structure evaluation. Herein, four different structural parameters, sphericity, pellet volume, pore volume and internal porosity were calculated by Image Pro Premier software at different time points. The total volume of compendium medium

entered the pellets was estimated from the pore volume. The structural changes in enteric coated pellets while passing through stomach are of great importance as they are designed to be protected in stomach environment. Hence, the two-tailed t-test was conducted on 3D structure quantitative parameters after 2 h between the *in vivo* and *in vitro* group.

In terms of sphericity for ESO and OME pellets, differences existed between *in vitro* compendium media and *in vivo* groups. It was discovered that the ESO pellets (Fig. 8A) maintained their sphericity *in vitro* compendium media while it was affected more *in vivo* showing a first increase with a subsequent decrease. After pepsin or GM addition, the sphericity of ESO pellets exhibited no significant differences between *in vitro and in vivo* (Fig. 8E). On the contrary, the sphericity of OME pellets deteriorated significantly with dilution time in all groups (Fig. 9A), which could be explained by the fact that the coating layer of the methacrylic acid copolymer was eroded and the hardness of the coating layer decreased over time. A big difference was recorded between *in vitro* compendium media group and the *in vivo* group ($P < 0.001$). However, this difference at 2 h diminished by pepsin addition ($P < 0.01$) and almost disappeared with GM or pepsin-GM addition (Fig. 9E).
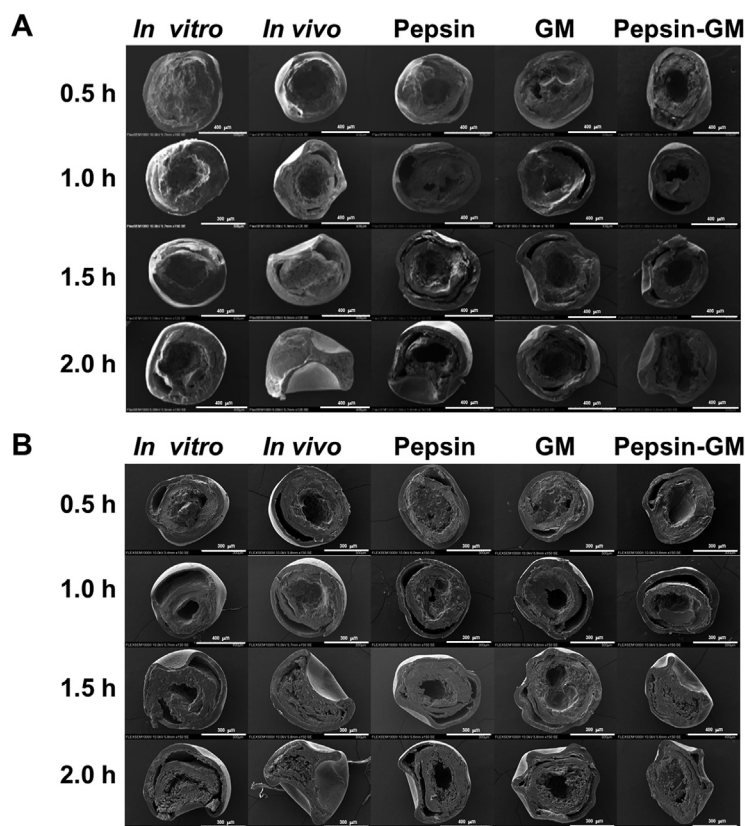
Figure 5 The 2D structure of ESO and OME pellets at different time points after optimization of dissolution conditions *via* SEM. (A) ESO pellets. (B) OME pellets.

For the pellet volume, it could be observed that the volume of ESO pellet *in vitro* compendium media kept increasing with time might be due to the swelling (Fig. 8B), which was also confirmed by CT imaging (Fig. 3). However, affected by the peristalsis and enzymatic effects in the stomach, the ESO pellets with original volume of 1.20×10^8 μm^3 reached to the maximum value of 1.76×10^8 μm^3 at 1 h then reduced to 1.55×10^8 μm^3 at 2 h. As shown in Fig. 8F, significant difference was presented between *in vitro* compendium media and *in vivo* experimental group, while the difference decreased when GM and pepsin addition. Differently, pellet volume of OME pellets showed the same fashion in both conditions, increased and then decreased but the magnitude and rate of the changes *in vivo* were significantly different from *in vitro* compendium media (Fig. 9B). This phenomenon may account for the reasons that the medium absorption and swelling effect were dominant in the early stage, whereas the erosion behavior took over in the later stage. After the introduction of pepsin or GM, the tendency of the pellet volume became consistent with that of *in vivo* samples.

Additionally, the total amount of media entered into pellet could be estimated from the pore volume. For the pristine ESO pellets, few pores formed during the preparation process were observed. Nevertheless, the internal porosity of pellets *in vitro* compendium media increased rapidly (250 times) within first 1 h and then slowly from 1 to 2 h indicating the fast penetration of media at first and then slowed down. In contrast, both the pore volume and the internal porosity of ESO pellets *in vivo* showed the tendency to increase (0.5−1 h), decrease (1−1.5 h) and again increase (1.5−2 h, Fig. 8C and D). The CT imaging results also confirmed that the pore volume of pellets *in vivo* indicated by the

arrows continually increased with time (Fig. 3). It could be interpreted as: initially, gastric acid penetrated into the intact pellet causing them to expand. With the retention of pellets in the stomach, the enteric coating layer became soft and the gastric peristalsis caused squeeze and deformations in pellets. Finally, due to the holes formed in the outermost coating layer, gastric acid continuously entered the pellets and further penetrated to the drug and the core. In comparison to ESO pellets at 0 h, the internal porosity of the pellets *in vivo* increased significantly by 404 times after 2 h. In line with the statistical analysis (Fig. 8G and H), except for the differences between pepsin-GM group and *in vivo* group ($P < 0.01$), significantly high statistical differences were recorded between other groups and *in vivo* group on the pore volume of ESO pellets ($P < 0.001$). For OME pellets, same parameters presented diverse changing pattern, including rising (0.5−1.5 h) and slightly falling (1.5−2 h) stages *in vitro* compendium media and obvious descending after increasing in the first hour *in vivo* (Fig. 9C and D). The differences could be attributed to the significant reductions in sphericity of OME pellets and volume as a result of mechanical extrusion and enzymatic effect, which were quite compatible with SR-μCT results (Fig. 4). In more detail (Fig. 9G and H), no significant difference was recorded in either pore volume or porosity of OME pellets between the pepsin-GM group and *in vivo* group ($P > 0.05$).

In brief, adding pepsin and GM to *in vitro* compendium media could imitate the *in vivo* conditions to a large extent (Figs. 8 and 9). Even though there were minor discrepancies, the results were broadly consistent with *in vivo* changes. Herein, the data of quantitative parameters analysis were pertinently matched with SR-μCT reconstructed results. Consequently, favorable structure
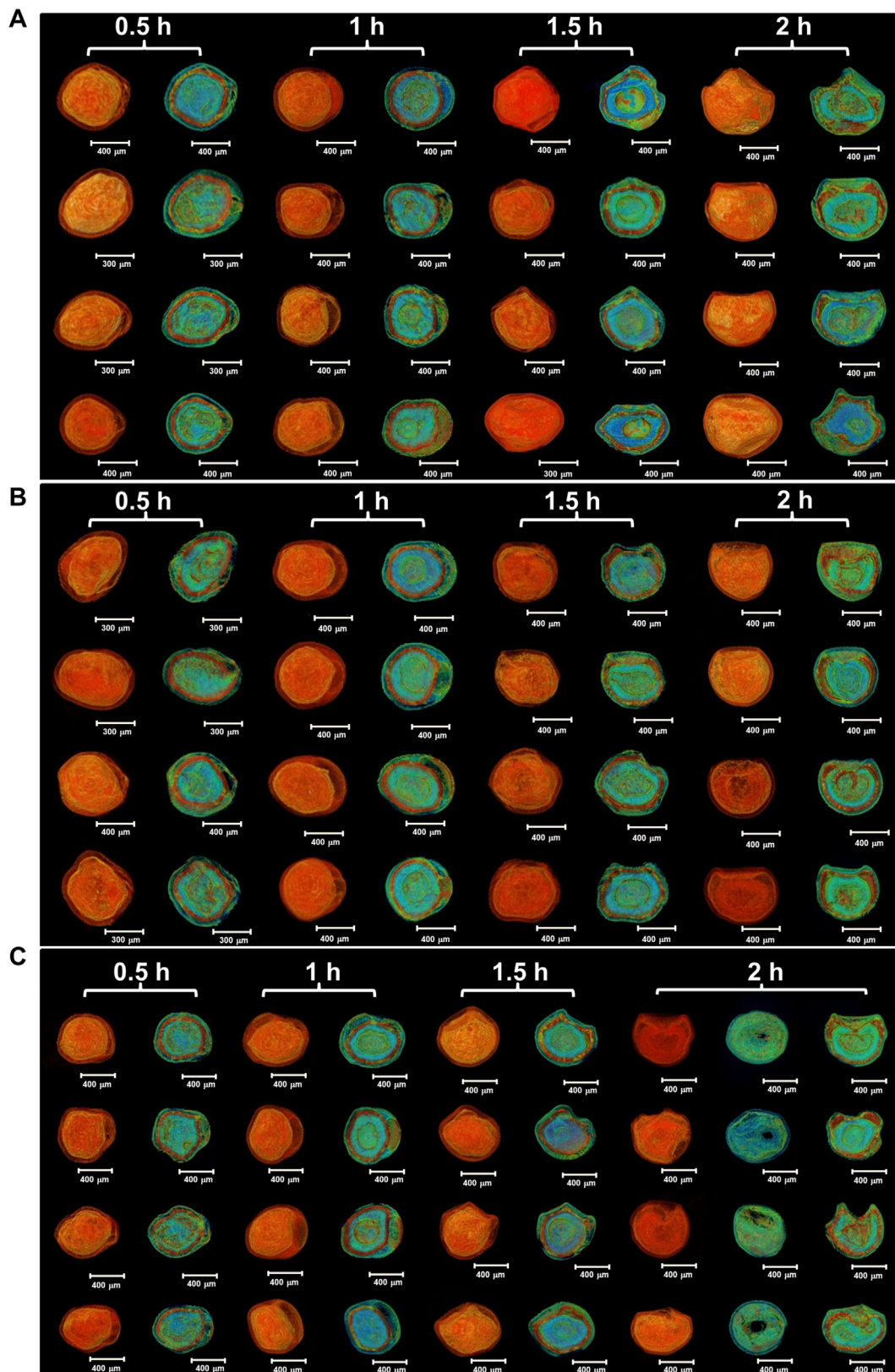
Figure 6   SR-μCT reconstructed 3D structure of ESO pellets with different dissolution conditions. Each time point contains two types of images: the transparent outer surface of the pellets (orange color) and the internal cross section of the pellets (multiple colors). (A) Structure of ESO pellets with pepsin added into the compendium media. (B) Structure of ESO pellets with GM added into the compendium media. (C) Structure of ESO pellets with pepsin-GM added into the compendium media.
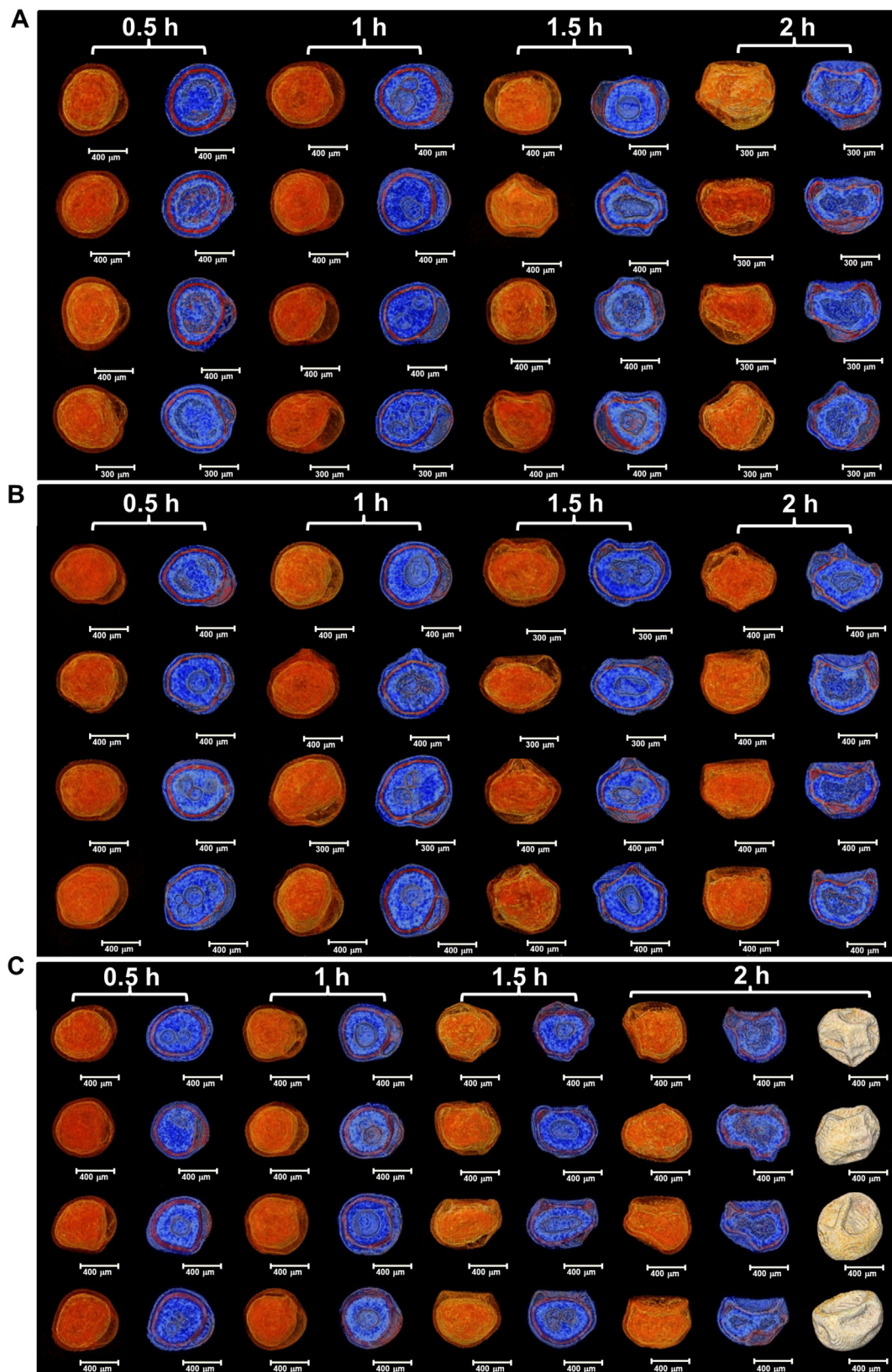
Figure 7 SR-µCT reconstructed 3D structure of OME pellets with different dissolution conditions. Each time point contains two types of images: the transparent outer surface of the pellets (orange color) and the internal cross section of the pellets (multiple colors). (A) Structure of OME pellets with pepsin added into the compendium media. (B) Structure of OME pellets with GM added into the compendium media. (C) Structure of OME pellets with pepsin-GM added into the compendium media.
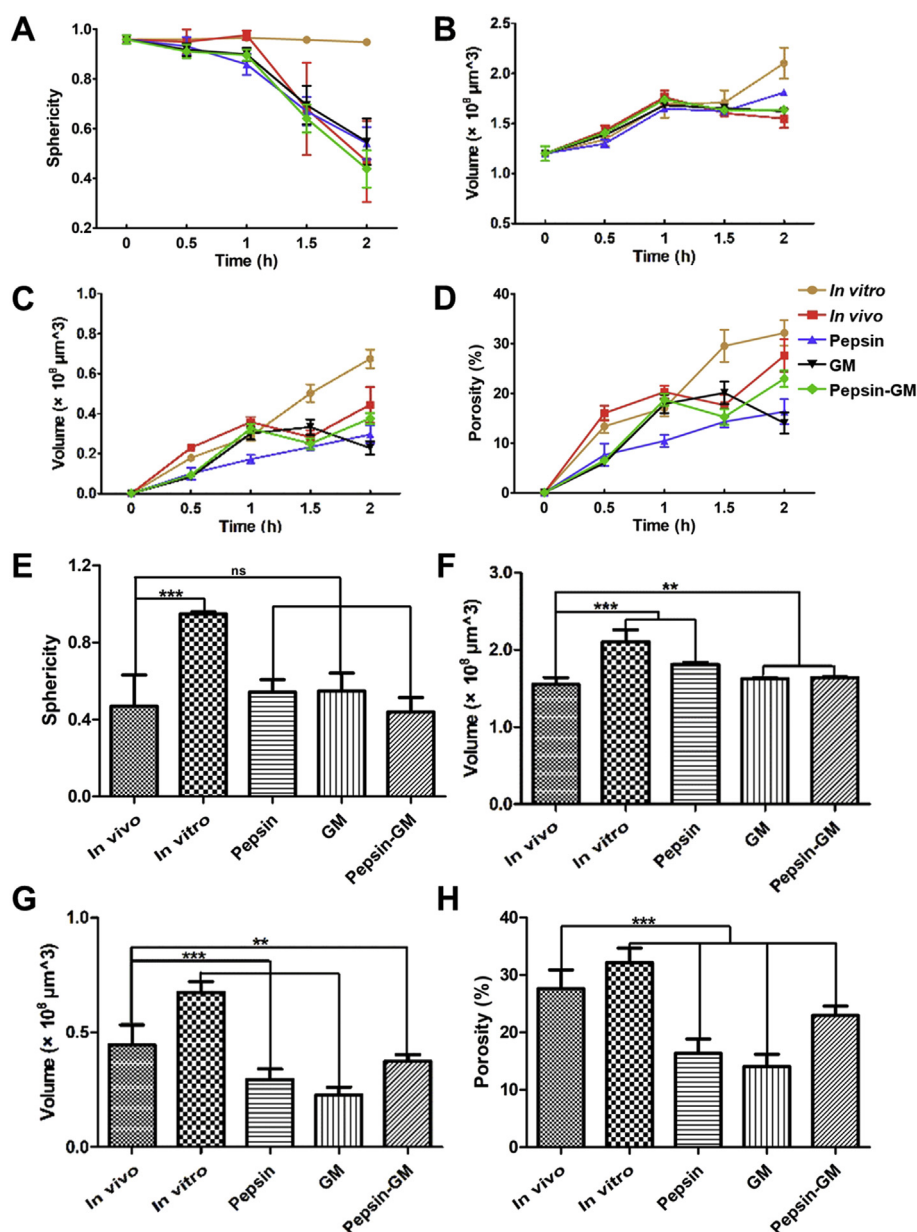
Figure 8 Comparison of 3D structure parameters of ESO pellets in five dissolution medias. (A) Sphericity within 2 h. (B) Pellet volume within 2 h. (C) Pore volume within 2 h. (D) Porosity within 2 h. (E) Statistical analysis of the sphericity of 2 h. (F) Statistical analysis of the pellet volume of 2 h. (G) Statistical analysis of the pore volume of 2 h. (H) Statistical analysis of the porosity of 2 h. Herein, *in vitro* means *in vitro* compendium media. Pepsin, GM and pepsin-GM represent the dissolution conditions for introducing pepsin, GM and pepsin-GM into the *in vitro* compendium media. Data are presented as mean $\pm$ SD ($n = 20$). *$P < 0.05$. **$P < 0.01$. ***$P < 0.001$. ns, not significant.

bridge between in compendium media and in gastro-intestinal tract of enteric coated pellets was established preliminarily. And more elaborated optimization requires further research to achieve complete *in vitro* and *in vivo* consistency.

4. Conclusions

In this research, SR-μCT was employed to visualize the structural changed in two different enteric coated pellets, both in compendium media and in gastrointestinal tract of rats. Diversities in structural characteristics of enteric coated pellets *in vitro* compendium media and *in vivo* were discovered in a way of 3D characterization. And the pellets structures in compendium media

and in gastro-intestinal tract were quantitatively correlated for the first time. Compared to the 3D structures of pellets in compendium media, the pellets *in vivo* showed poor integrity. Furthermore, the pellets *in vivo* exhibited worse sphericity, larger pore volume and higher porosity than pellets in a conventional HCl dissolution media due to the presence of enzymes and peristalsis in the former case. Being aware of this variance, optimization in the *in vitro* dissolution conditions were implemented through introduction of pepsin and GM into the compendium media. The pellets exhibited similar performance between *in vitro* compendium media and *in vivo*. Ultimately, the structural dynamic behaviors and structural parameters of the pellets *in vivo* and *in vitro* were observed almost identical and aligned, which showed the successful bridging of both the methods/environments. These
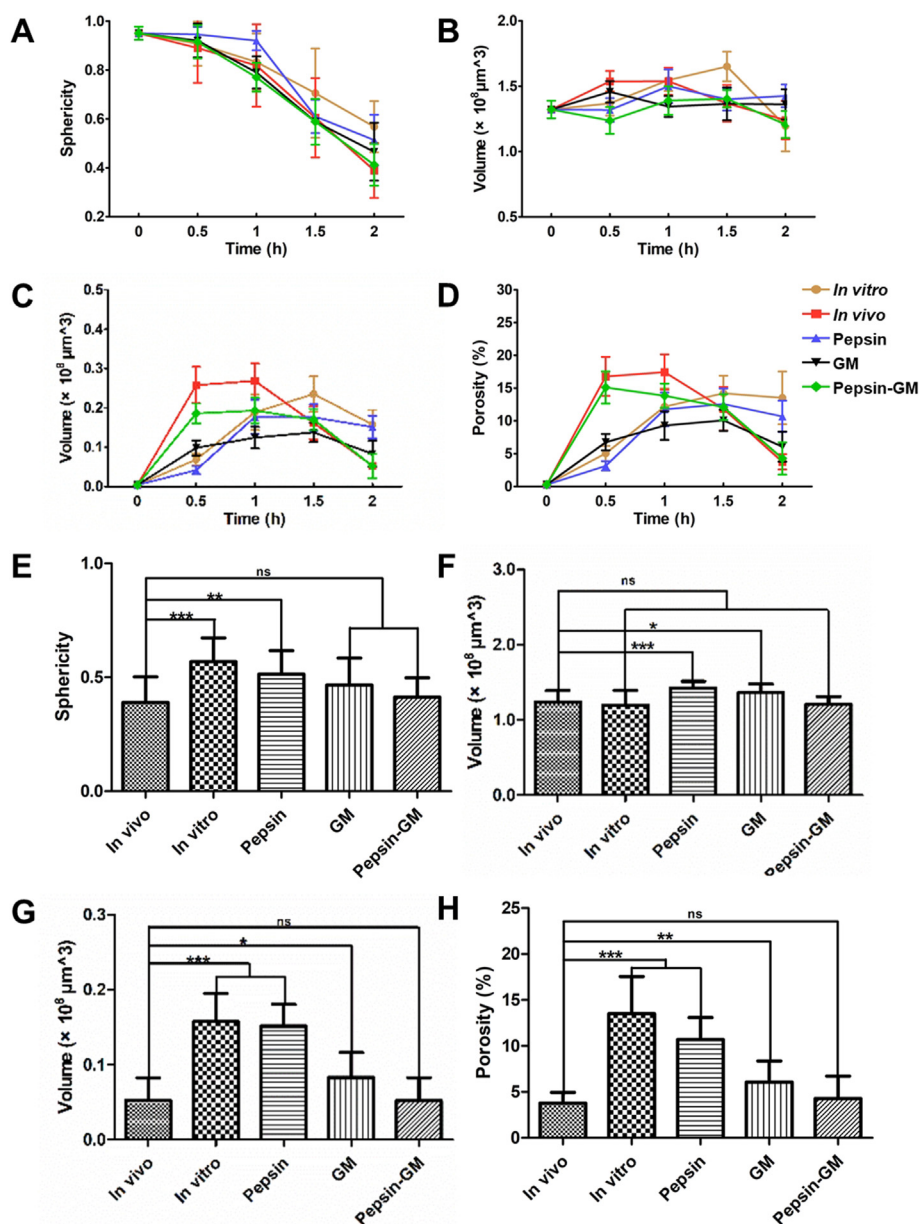
Figure 9 Comparison of 3D structure parameters of OME pellets in five dissolution medias. (A) Sphericity within 2 h. (B) Pellet volume within 2 h. (C) Pore volume within 2 h. (D) Porosity within 2 h. (E) Statistical analysis of the sphericity of 2 h. (F) Statistical analysis of the pellet volume of 2 h. (G) Statistical analysis of the pore volume of 2 h. (H) Statistical analysis of the porosity of 2 h. Data are presented as mean ± SD ($n = 20$). *$P < 0.05$. **$P < 0.01$. ***$P < 0.001$. ns, not significant.

findings are of particular importance to reconsider the existing *in vitro* characterizations and set a fundament for structure-based evaluation of advanced OSDF and guidance for the quality control of enteric-coated pellets. More importantly, these findings on the structural variation in pellets during dissolution stages will provide a new idea for the reverse engineering and development of the formulation process.

Author contributions

Jiwen Zhang, Xianzhen Yin and Li Wu designed the research. Hongyu Sun and Siyu He performed the experiments and contributed equally to this manuscript. Hongyu Sun completed the

pretreatment of imaging pellets and the collection of CT projections assisted by Mingwei Xu and Shan Lu. Hongyu Sun, Zeying Cao and Xian Sun performed the structural reconstruction and quantification of pellets. Siyu He, Mingdi Xu, Baoming Ning, Huimin Sun, Tiqiao Xiao, Peter York, Xu Xu, Jiwen Zhang revised the manuscript. All of the authors have read and approved the final manuscript.

Conflicts of interest

The authors declare no conflict of interest.

Appendix A.   Supporting information

Supporting data to this article can be found online at https://doi.org/10.1016/j.apsb.2021.05.010.

References

1. Guo Z, Yin XZ, Liu CB, Wu L, Zhu WF, Shao Q, et al. Microstructural investigation using synchrotron radiation X-ray microtomography reveals taste-masking mechanism of acetaminophen microspheres. *Int J Pharm* 2016;**499**:47−57.

2. Husted CA, Duijn JH, Matson GB, Maudsley AA, Weiner MW. Molar quantitation of *in vivo* proton metabolites in human brain with 3D magnetic resonance spectroscopic imaging. *Magn Reson Imaging* 1994;**12**:661−7.

3. Schregel K, Wuerfel E, Garteiser P, Gemeinhardt I, Prozorovski T, Aktas O, et al. Demyelination reduces brain parenchymal stiffness quantified *in vivo* by magnetic resonance elastography. *Proc Natl Acad Sci U S A* 2012;**109**:6650−5.

4. Furrer P, Gurny R. Recent advances in confocal microscopy for studying drug delivery to the eye: concepts and pharmaceutical applications. *Eur J Pharm Biopharm* 2010;**74**:33−40.

5. Markl D, Wang P, Ridgway C, Karttunen AP, Chakraborty M, Bawuah P, et al. Characterization of the pore structure of functionalized calcium carbonate tablets by terahertz time-domain spectroscopy and X-ray computed microtomography. *J Pharm Sci* 2017;**106**:1586−95.

6. Tafti AP, Kirkpatrick AB, Holz JD, Owen HA, Yu Z. 3Dsem: a 3D microscopy dataset. *Data Brief* 2016;**6**:112−6.

7. Houle MA, Burruss RC, Ridsdale A, Moffatt DJ, Légaré F, Stolow A. Rapid 3D chemical-specific imaging of minerals using stimulated Raman scattering microscopy. *J Raman Spectrosc* 2017;**48**:726−35.

8. Yoneyama A, Takeda T, Tsuchiya Y, Wu J, Lwin TT, Hyodo K. Coherence-contrast X-ray imaging based on X-ray interferometry. *Appl Opt* 2005;**44**:3258−61.

9. Qi JC, Ye LL, Chen RC, Xie HL, Ren YQ, Deng B, et al. Coherence of X-ray in the third synchrotron radiation source. *Acta Phys Sin* 2014;**63**:104202.

10. Li HY, Yin XZ, Ji JQ, Sun LX, Shao Q, York P, et al. Microstructural investigation to the controlled release kinetics of monolith osmotic pump tablets *via* synchrotron radiation X-ray microtomography. *Int J Pharm* 2012;**427**:270−5.

11. Fang LW, Yin XZ, Wu L, He YP, He YZ, Qin W, et al. Classification of microcrystalline celluloses *via* structures of individual particles measured by synchrotron radiation X-ray micro-computed tomography. *Int J Pharm* 2017;**531**:658−67.

12. Jannin V, Leccia E, Rosiaux Y, Doucet J. Evolution of the microstructure of sustained-release matrix tablets during dissolution and storage. *Indian J Pharmaceut Sci* 2018;**80**:1011.

13. Wu L, Wang ML, Singh V, Li HY, Guo Z, Gui SY, et al. Three dimensional distribution of surfactant in microspheres revealed by synchrotron radiation X-ray microcomputed tomography. *Asian J Pharm Sci* 2017;**12**:326−34.

14. Yin XZ, Wu L, Li Y, Guo T, Li HY, Xiao TQ, et al. Visualization and quantification of deformation behavior of clopidogrel bisulfate polymorphs during tableting. *Sci Rep* 2016;**6**:21770.

15. Yin XZ, Li L, Gu XQ, Wang HM, Wu L, Qin W, et al. Dynamic structure model of polyelectrolyte complex based controlled-release matrix tablets visualized by synchrotron radiation microcomputed tomography. *Mater Sci Eng C Mater Biol Appl* 2020;**116**:111137.

16. Yin XZ, Xiao TQ, Nangia A, Yang S, Lu XL, Li HY, et al. *In situ* 3D topographic and shape analysis by synchrotron radiation X-ray microtomography for crystal form identification in polymorphic mixtures. *Sci Rep* 2016;**6**:24763.

17. Yin XZ, Li HY, Guo Z, Wu L, Chen FW, de Matas M, et al. Quantification of swelling and erosion in the controlled release of a poorly water-soluble drug using synchrotron X-ray computed microtomography. *AAPS J* 2013;**15**:1025−34.

18. Yang S, Yin XZ, Wang CF, Li HY, He Y, Xiao TQ, et al. Release behaviour of single pellets and internal fine 3D structural features co-define the *in vitro* drug release profile. *AAPS J* 2014;**16**:860−71.

19. Zhang L, Wu L, Wang CF, Zhang GQ, Yu L, Li HY, et al. Synchrotron radiation micro-computed tomography-guided chromatographic analysis displays the material distribution in tablets. *Anal Chem* 2018;**90**:3238−44.

20. Sun X, Wu L, Maharjan A, Sun HY, Hu XX, York P, et al. Static and dynamic structural features of single pellets determine the release behaviors of metoprolol succinate sustained-release tablets. *Eur J Pharmaceut Sci* 2020;**149**:105324.

21. Bodmeier R. Tableting of coated pellets. *Eur J Pharm Biopharm* 1997;**43**:1−8.

22. Patel S, Patel N, Misra M, Joshi A. Controlled-release domperidone pellets compressed into fast disintegrating tablets forming a multiple-unit pellet system (mups). *J Drug Deliv Sci Technol* 2018;**45**:220−9.

23. Osei-Yeboah F, Lan Y, Sun CC. A top coating strategy with highly bonding polymers to enable direct tableting of multiple unit pellet system (mups). *Powder Technol* 2017;**305**:591−6.

24. Zhao YN, Zeng CL, Liu JP, Zhu JB. Advance in tableting of coated pellets. *Chin J New Drugs* 2012;**21**:2287−91.

25. Chen TK, Li J, Chen T, Sun CC, Zheng Y. Tablets of multi-unit pellet system for controlled drug delivery. *J Control Release* 2017;**262**:222−31.

26. Abdul S, Poddar SS. A flexible technology for modified release of drugs: multi layered tablets. *J Control Release* 2004;**97**:393−405.

27. Bauer K, Kesselhut J. Novel pharmaceutical excipients for colon targeting. *STP Pharma Sci* 1995;**5**:54−9.

28. Bergstrand PJA, Lövgren KI, inventors; AstraZeneca AB (SE), assignee. Multiple unit tableted dosage form. European Patent EP1078628. 2001 Nov 19.

29. Combessis D, Corvaisier D, Alexandre G, Guerin E, inventors; AstraZeneca AB (SE), assignee. Pharmaceutical multiparticulate tablet formulations and process for their preparation. European Patent EP1621187. 2006 Feb 1.

30. Bergstrand P, Wang P, inventors; AstraZeneca AB (SE), assignee. Pharmaceutical formulation comprising omeprazole. United States Patent US No. 6428810. 2002 Aug 6.